

# APPROACH TO HIGH-DENSITY NUCLEAR MATTER VIA NUCLEUS–NUCLEUS ELASTIC SCATTERING\*

T. FURUMOTO

National Institute of Technology, Ichosenoki College  
Ichinoseki, Iwate 021-8511, Japan

Y. SAKURAGI

Department of Physics, Osaka City University, Osaka 558-8585, Japan

Y. YAMAMOTO

RIKEN Nishina Center, Wako, Saitama 351-0198, Japan

*(Received November 25, 2015)*

We investigate the effect of the high-density nuclear matter on the nucleus–nucleus elastic scattering in the framework of the double-folding (DF) model with the complex  $G$ -matrix interaction. The medium effect including three-body-force (TBF) effect described by the multi-Pomeron exchange potential is investigated with the present methods. One of the methods is to control the medium effect by changing the local density in the DF model calculation. The other is to replace the complex  $G$ -matrix interaction with the TBF effect by that without the TBF effect in the calculation. With both methods, it is made clear that the heavy-ion elastic scattering is very sensitive to the medium effects in the high-density region. Finally, we make clear the crucial role of the TBF effect up to  $k_F = 1.6 \text{ fm}^{-1}$  in the nucleus–nucleus elastic scattering.

DOI:10.5506/APhysPolB.47.853

## 1. Introduction

The construction of the reaction potential from the microscopic view point is one of key issues for the nuclear physics not only to analyze the nuclear reaction data but also to understand nuclear reaction mechanism and fundamental interactions between complex nuclear systems. In order to construct the complex potential for the heavy-ion system, the complex

---

\* Presented at the XXXIV Mazurian Lakes Conference on Physics, Piaski, Poland, September 6–13, 2015.

$G$ -matrix interactions have been widely applied to the double-folding (DF) model [1–5]. Recently, the present authors proposed the complex  $G$ -matrix interaction, CEG07 [6, 7], whose density dependence is calculated up to twice the normal density ( $k_F = 1.8 \text{ fm}^{-1}$ ) for the DF model based on the frozen-density approximation (FDA). By the FDA, the medium effect including the TBF effect in the complex  $G$ -matrix interaction can be investigated up to twice the normal density. Then, they have applied the CEG07 interaction to the DF model, and the DF potential with the CEG07 interaction well reproduces the experimental data of the nucleus–nucleus elastic scattering and the important role of the three-body force (TBF) effect, which is included in the CEG07 interaction, on the heavy-ion scattering is made clear [7–9]. In Ref. [10], the TBF effect introduced by a multi-Pomeron exchange potential (MPP) was given more clearly. The MPP model includes triple and quartic Pomeron exchanges, and can lead to the neutron-star EOS stiff enough to reproduce a maximum star mass over  $2M_\odot$  [11].

In this paper, we apply the complex  $G$ -matrix interaction, which is called MPa interaction based on the nucleon–nucleon ( $NN$ ) ESC08 interaction with the MPP model [12, 13] to the DF model calculation. In the DF model, it is considered that the local density through the FDA reaches up to about twice the normal density. We here clarify the decisive role of the medium effect, including the TBF effect, in such high-density system on the DF potential and scattering observables of the nucleus–nucleus system. To this end, we demonstrate the importance of properly evaluating the medium effect at high-density region to a sufficient convergence of the calculated DF potential in the spatial region that can be proved by the observed elastic scattering cross sections.

## 2. Formalism

We construct the nucleus–nucleus potential based on the DF model with the use of the complex  $G$ -matrix interaction including the TBF effect based on the MPP model. The microscopic nucleus–nucleus potential can be written as follows:

$$U_D(R) = \int \rho_1(\mathbf{r}_1)\rho_2(\mathbf{r}_2)v_D(s; \rho, E/A)d\mathbf{r}_1d\mathbf{r}_2, \quad (1)$$

where  $\mathbf{s} = \mathbf{r}_2 - \mathbf{r}_1 + \mathbf{R}$ , and

$$U_{EX}(R) = \int \rho_1(\mathbf{r}_1, \mathbf{r}_1 + \mathbf{s})\rho_2(\mathbf{r}_2, \mathbf{r}_2 - \mathbf{s})v_{EX}(s; \rho, E/A) \\ \times \exp\left[\frac{i\mathbf{k}(R) \cdot \mathbf{s}}{M}\right]d\mathbf{r}_1d\mathbf{r}_2. \quad (2)$$

Here,  $U_D$  and  $U_{EX}$  are the direct and exchange parts of the DF model potential, respectively.  $v_D$  and  $v_{EX}$  are the complex  $G$ -matrix interaction for the direct and exchange parts, respectively.  $\rho_1$  and  $\rho_2$  are the projectile and target densities, respectively.  $\rho(\mathbf{r}, \mathbf{r}')$  is the density matrix.  $E/A$  is the incident energy per nucleon.  $\mathbf{k}(R)$  is the local momentum for nucleus–nucleus relative motion. The detailed procedure of the calculations is given in Ref. [14] and references therein.

In the present calculations, we employ the FDA for the local density as mentioned in the introduction. In the FDA, the density-dependent  $NN$  interaction is assumed to feel the local density defined as the sum of densities of colliding nuclei evaluated

$$\rho = \rho_1(\mathbf{r}_1) + \rho_2(\mathbf{r}_2). \tag{3}$$

The FDA has been widely used also in the standard DF model calculations [15–19]. In Ref. [7], it is confirmed that FDA is the best prescription in the case with complex  $G$ -matrix interaction to reproduce the data.

We investigate the medium effect for the high-density region in the framework of the DF model with complex  $G$ -matrix interaction. Then, we test the sensitivity of the medium effect in the high-density region by the following artificial cut of the evaluated local density:

$$\rho = \begin{cases} \rho_1 + \rho_2 & \dots \text{ (if } \rho_1 + \rho_2 < \rho_{\text{cut}}) \\ \rho_{\text{cut}} & \dots \text{ (if } \rho_1 + \rho_2 > \rho_{\text{cut}}) \end{cases}, \tag{4}$$

where the  $\rho_{\text{cut}}$  value is varied as a parameter. In addition, we here test the sensitivity of the TBF effect in the high-density region by the following prescription for the complex  $G$ -matrix interaction:

$$v(\mathbf{s}; \rho, E/A) = \begin{cases} \text{MPa} & \text{(with TBF)} \\ \dots & \text{(if } \rho = \rho_1 + \rho_2 < \rho_{\text{rep}}), \\ \text{ESC} & \text{(w/o TBF)} \\ \dots & \text{(if } \rho = \rho_1 + \rho_2 > \rho_{\text{rep}}), \end{cases} \tag{5}$$

where the ESC interaction is the complex  $G$ -matrix interaction constructed only from the ESC08 interaction. Namely, the ESC interaction does not include the TBF effect. The  $\rho_{\text{rep}}$  is also the parameter. We calculate the DF potentials with several  $k_{\text{cut,rep}}$  values, where  $k_{\text{cut,rep}}$  is defined by

$$\rho_{\text{cut,rep}} = \frac{2}{3\pi^2} k_{\text{cut,rep}}^3. \tag{6}$$

By changing the  $k_{\text{cut,rep}}$  values, the medium effect including the TBF effect in the high-density region is controlled and investigated in the potential and the corresponding elastic cross sections.

### 2.1. Results

We adopt the nucleon density of the  $^{16}\text{O}$  nucleus calculated from the internal wave functions generated by the orthogonal condition model (OCM) by Okabe [20] based on the microscopic  $\alpha + ^{12}\text{C}$  cluster picture.

Figure 1 shows the real and imaginary parts of the calculated DF potential for the  $^{16}\text{O} + ^{16}\text{O}$  elastic scattering at  $E/A = 70$  MeV. The medium effect including the TBF effect over the normal density is clearly seen in both potentials. The medium effect by the  $G$ -matrix calculation suppresses the inner part of the potentials as described with the bold curves. Moreover,

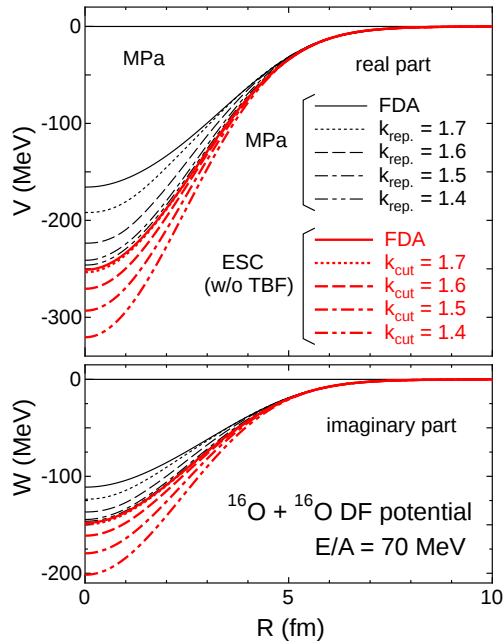


Fig. 1. The real and imaginary parts of the DF potential with the  $k_{\text{cut}}$  and  $k_{\text{rep}}$  values. The black and bold solid curves are the DFM potential based on the FDA with the MPA (with TBF) and ESC (w/o TBF) interactions. The dotted, dashed, dot-dashed and dot-dot-dashed curves are the results of the MPA interaction with  $k_{\text{rep}} = 1.7, 1.6, 1.5$  and  $1.4$  ( $\text{fm}^{-1}$ ), respectively. The bold dotted, dashed, dot-dashed and 2 dots-dashed curves are the results of the ESC interaction with  $k_{\text{cut}} = 1.7, 1.6, 1.5$  and  $1.4$  ( $\text{fm}^{-1}$ ), respectively.

the TBF effect by the MPP also suppresses the inner part of the potentials (thin curves). Figure 2 shows the results calculated with the DF potentials shown in Fig. 1 for the  $^{16}\text{O} + ^{16}\text{O}$  elastic scattering at  $E/A = 70$  MeV. When the TBF effect is not included, the medium effect is obtained only by the  $G$ -matrix calculation. This effect is not enough to reproduce the elastic

cross section as shown by the bold curves. The crucial role of the TBF effect described by the thin curves is clearly seen in the cross section. Especially, the TBF effect in the high-density region ( $k_F \geq 1.4 \text{ fm}^{-1}$ ) has a crucial role to reproduce the data. In addition, the TBF effect is clearly seen up to  $k_F = 1.6 \text{ fm}^{-1}$  in the elastic cross section. This result implies that the nucleus–nucleus elastic scattering is a good candidate to probe the important role of the TBF effect in the high-density region up to  $k_F = 1.6 \text{ fm}^{-1}$ .

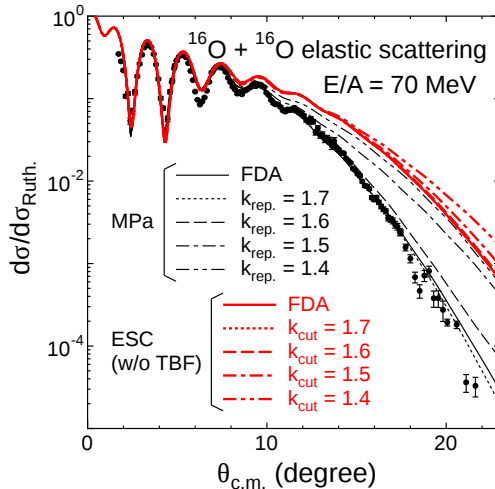


Fig. 2. The medium effect in the high-density region on the elastic cross section. The meaning of the curves is the same as in Fig. 1. The experimental data are taken from Ref. [21].

## 2.2. Summary and remark

In summary, we have constructed the DF potential with the complex  $G$ -matrix interaction with and without the TBF effect based on the MPP model. With the  $k_{\text{cut,rep}}$  values, the medium effect including the TBF effect is investigated in the potential and the elastic cross section. The medium effect is clearly seen. Especially, the TBF effect up to  $k_F = 1.6 \text{ fm}^{-1}$  has a critical role to determine the elastic angular distribution. This result implies that the medium effect, especially the TBF effect, in the high-density region can be probed by the measured elastic scattering. Finally, we made clear the crucial role of the TBF effect in the high-density region on the nucleus–nucleus elastic scattering.

This work is supported by the JSPS KAKENHI Grant Number 15H00842.

## REFERENCES

- [1] S. Nagata, M. Kamimura, N. Yamaguchi, *Prog. Theor. Phys.* **73**, 512 (1985).
- [2] F. Carstoiu, M. Lassau, *Nucl. Phys. A* **597**, 269 (1996).
- [3] L. Trache *et al.*, *Phys. Rev. C* **61**, 024612 (2000).
- [4] J.C. Blackmon, *et al.*, *Phys. Rev. C* **72**, 034606 (2005).
- [5] T. Furumoto, Y. Sakuragi, *Phys. Rev. C* **74**, 034606 (2006).
- [6] T. Furumoto, Y. Sakuragi, Y. Yamamoto, *Phys. Rev. C* **78**, 044610 (2008).
- [7] T. Furumoto, Y. Sakuragi, Y. Yamamoto, *Phys. Rev. C* **80**, 044614 (2009).
- [8] T. Furumoto, Y. Sakuragi, Y. Yamamoto, *Phys. Rev. C* **79**, 011601(R) (2009).
- [9] T. Furumoto *et al.*, *Phys. Rev. C* **85**, 044607 (2012).
- [10] Y. Yamamoto, T. Furumoto, N. Yasutake, T.A. Rijken, *Phys. Rev. C* **88**, 022801(R) (2013).
- [11] Y. Yamamoto, T. Furumoto, N. Yasutake, T.A. Rijken, *Phys. Rev. C* **90**, 045805 (2014).
- [12] T.A. Rijken, M.M. Nagels, Y. Yamamoto, *Prog. Theor. Phys. Suppl.* **185**, 14 (2010).
- [13] T.A. Rijken, M.M. Nagels, Y. Yamamoto, in: Proc. of the International Workshop on Strangeness Nuclear Physics, 2012 [Genshikaku Kenkyu 57 (Suppl. 3), 6 (2013)].
- [14] T. Furumoto, Y. Sakuragi, Y. Yamamoto, *Phys. Rev. C* **90**, 041601(R) (2014).
- [15] G.R. Satchler, W.G. Love, *Phys. Rep.* **55**, 183 (1979).
- [16] D.T. Khoa, W. von Oertzen, H.G. Bohlen, *Phys. Rev. C* **49**, 1652 (1994).
- [17] D.T. Khoa, G.R. Satchler, W. von Oertzen, *Phys. Rev. C* **56**, 954 (1997).
- [18] D.T. Khoa, *Phys. Rev. C* **63**, 034007 (2001).
- [19] M. Katsuma, Y. Sakuragi, S. Okabe, Y. Kondo, *Prog. Theor. Phys.* **107**, 377 (2002).
- [20] S. Okabe, in: Tours Symposium on Nuclear Physics II, Eds. H. Utsunomiya, M. Ohta, J. Galin, G. Münzenberg, World Scientific, Singapore 1995, p. 112.
- [21] F. Nuoffer *et al.*, *Nuovo Cim. A* **111**, 971 (1998).